Simultaneous *Q*-Switching of a Tm^{3+}:ZBLAN Fiber Laser at 1.9 μm and 2.3 μm Using Graphene

Chenglai Jia, Bhavin J. Shastri, *Member, IEEE*, Paul R. Prucnal, *Fellow, IEEE*, Mohammed Saad, and Lawrence R. Chen, *Senior Member, IEEE*

***Abstract*— We demonstrate a passively *Q*-switched, dual-band Tm^{3+}:ZBLAN fiber laser operating simultaneously around 1895 and 2315 nm using bidirectional pumping at 795 nm and a graphene saturable absorber. The *Q*-switched pulse trains at 1895 and 2315 nm have a synchronized repetition rate from 10.8 to 25.2 kHz with pulse durations as short as 4.5 and 4.9 μs, respectively.**

***Index Terms*— Thulium-doped ZBLAN fiber, fiber lasers, *Q*-switched lasers, graphene, mid-infrared lasers.**

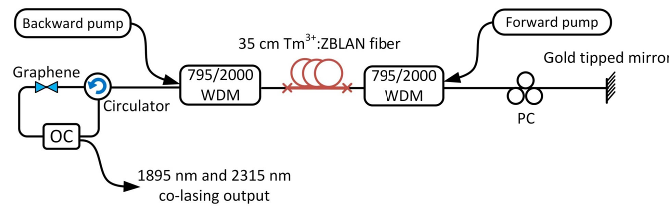

Fig. 1. Graphene-based *Q*-switched Tm^{3+}:ZBLAN all fiber laser configuration.

I. INTRODUCTION

THULIUM-DOPED ZBLAN (Tm^{3+}:ZBLAN) fiber is an excellent rare-earth doped fiber to generate lasing operation covering from ultra-violet to mid-infrared regions due to its unique advantages such as low phonon energy, high stability, and ultra-broadband transparency [1], [2]. Compared with a silica host, the ZBLAN host has a reduced multi-phonon emission rate and a longer radiative lifetime of the upper laser level, especially for the $^3F_4 \rightarrow {}^3H_5$ transition with resulting emission around 2300 nm [3]. In addition, the $^3H_4 \rightarrow {}^3H_6$ transition with resulting emission around 1900 nm can be further improved by the simultaneous laser oscillation around 2300 nm to increase the branching ratio from $^3F_4$ to $^3H_4$ [4], [5]. There have been several reports of continuous-wave (CW) co-lasing at 1900 nm and 2300 nm in Tm^{3+}:ZBLAN fiber [3], [4], [6], [7] along with demonstrated applications in gas sensing [3].

Q-switching is a technique to modulate the quality factor of a laser cavity for the generation of high energy nanosecond pulses. Compared with actively *Q*-switched fiber lasers, passively *Q*-switched configurations have unique advantages such as simplicity, compactness, ease of integration, and low cost. Recently, graphene has emerged as an innovative and promising material as a saturable absorber (SA) for passive pulse generation in fiber lasers due to its remarkable optical properties such as high saturable absorption to volume ratio, ultra-broadband frequency tunability, very fast response time, tunable modulation depth, and high optical damage threshold [8], [9]. Previously, graphene has been successfully used to realize *Q*-switched ZBLAN fiber lasers. For example, using graphene SAs, passively *Q*-switched ZBLAN fiber lasers have been demonstrated at ∼1190 nm and ∼3000 nm with Ho^{3+}:ZBLAN fiber [10], [11], and at ∼2780 nm with Er^{3+}:ZBLAN fiber [12]. Recently, we reported a passively synchronized *Q*-switched fiber laser at ∼1480 nm and ∼1840 nm using Tm^{3+}:ZBLAN fiber and a graphene SA [13]. Li *et al.* also presented dual-band pulsing at ∼2000 nm and ∼3000 nm using Ho^{3+}:ZBLAN fiber with a combination of gain-switching and *Q*-switching [14]. To date, there have been no reports of dual-band *Q*-switched laser sources with simultaneous operation at 1900 nm and 2300 nm in a single, all-fiber cavity. Such sources can add new capabilities for providing high energy nanosecond pulses for signal processing in the newly exploited optical transmission window around 2000 nm [15] or for sensing and gas concentration detection [2], [3].

In this letter, we demonstrate a passively *Q*-switched Tm^{3+}:ZBLAN all-fiber laser at ∼1900 nm and ∼2300 nm using a graphene SA. Using bidirectional pumping at 795 nm, simultaneous *Q*-switching operation is obtained with a synchronized repetition rate from 10.8 kHz to 25.2 kHz, and pulse durations as short as 4.5 μs at 1895 nm and 4.9 μs at 2315 nm.

II. EXPERIMENTAL SETUP

Fig. 1 shows the schematic of our passively *Q*-switched Tm^{3+}:ZBLAN all fiber laser at 1895 nm and 2315 nm using a graphene SA. We adopt a bidirectional pumping scheme with two 795 nm multi-mode laser diodes in a linear cavity configuration. The pump and lasing signals are coupled using two 795/2000 nm wavelength division multiplexers (WDMs). The linear laser cavity is defined by one gold-tipped mirror on one end and a loop mirror on the other. The gain medium

Manuscript received November 8, 2016; revised December 19, 2016; accepted January 6, 2017. Date of publication January 10, 2017; date of current version February 1, 2017. This work was supported in part by the Natural Sciences and Engineering Research Council of Canada.

C. Jia and L. R. Chen are with the Department of Electrical and Computer Engineering, McGill University, Montréal, Québec H3A 0E9, Canada (e-mail: lawrence.chen@mcgill.ca).

B. J. Shastri and P. R. Prucnal are with the Department of Electrical Engineering, Princeton University, Princeton, NJ 08544 USA.

M. Saad is with Thorlabs, Inc., Newton, NJ 07860 USA.

Color versions of one or more of the figures in this letter are available online at http://ieeexplore.ieee.org.

Digital Object Identifier 10.1109/LPT.2017.2650951

is a 35 cm length of double cladding (DC) Tm^{3+}:ZBLAN fiber manufactured by IRphotonics/Thorlabs Inc. with a doping concentration of 8,000 ppm Tm^{3+} ions and a numerical aperture (NA) of 0.13 (in separate experiments, we found that 35 cm was optimal in terms of maximizing the amplified spontaneous emission (ASE) output and spectral distribution for operation at both 1900 nm and 2300 nm); the core diameter is 8 μm and the cladding diameter is 125 μm coated with 15 μm of mixed fluoroacrylate and acrylate. When 800 mW of pump power at 795 nm is launched into the 35 cm length of gain fiber, the residual power at the output is ~10 mW. The Tm^{3+}:ZBLAN fiber is coupled with the DC silica fiber (FUD4070, Nufern) from two WDMs through a pair of glue splices (represented by × in Fig. 1). A polarization controller (PC) with SM2000 fiber is used to adjust the intra-cavity polarization and to optimize the laser output. A circulator, a graphene SA, and an optical coupler (OC) constitute the loop mirror and are all based on SMF28 fiber. The circulator has a transmission loss of ~0.5 dB around 1900 nm and ~1.5 dB around 2300 nm, and forces the signal to propagate counter-clockwise. The graphene film is deposited and sandwiched between two FC/APC connectors to form the SA. The preparation of the graphene film is described in detail in [16] and uses a similar process to that in [17]. Characterization of the samples shows that they comprise a few layers (typically 6) of graphene; moreover, the modulation depth is 40% - 50% and the saturation intensity is ~0.7 MW/cm^2 at 1550 nm (we do not have corresponding values of modulation depth and saturation intensity at 1900 nm or 2300 nm due to the lack of suitable sources at these wavelengths, apart from the laser developed and reported here). The laser output is extracted from the 10% port of the OC. The total cavity length of the Q-switched all-fiber laser is ~24.5 m and the estimated cavity loss is ~14 dB.

The optical spectrum is measured by an optical spectrum analyzer (OSA, YOKOGAWA, AQ6375) with a wavelength range from 1200 nm to 2400 nm and a resolution bandwidth of 0.05 nm. In order to characterize the Q-switched pulses at each wavelength, two bandpass filters around 1900 nm and 2300 nm are separately applied before the laser output to isolate the desired pulses. The temporal pulse trains are measured by a combination of a 7 GHz photodetector (Newport, 818-BB-51F) and a 60 MHz digital oscilloscope (Agilent, 54621A). The RF spectrum is monitored by an electrical spectrum analyzer (ESA, Anritsu, MS2668C) with a frequency range from 9 kHz to 40 GHz. Output powers are measured by a power meter (Thorlabs, PM10,D) and a thermal power sensor (Thorlabs, S302C) with a sensitivity of 1 μW. Note that all the pump power measurements refer to those after the WDM couplers. In order to protect the glue splicing between the Tm^{3+}:ZBLAN and SM2000 fiber, the maximum forward and backward pump powers used are 1000 mW.

III. Results and Discussion

Fig. 2(a) shows the operating regimes of the fiber laser including CW and Q-switched operation at 1895 nm and 2315 nm as functions of the bidirectional pump powers. Since the optical coupler and circulator are not optimized for

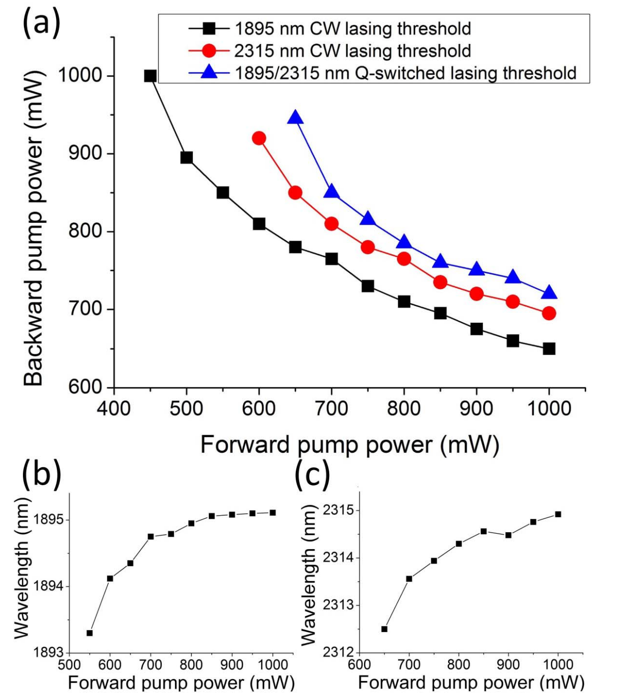

Fig. 2. (a) Lasing operation regimes (CW and Q-switched) as functions of forward and backward pump powers. Variation in lasing wavelength at (b) ~1895 nm and (c) ~2315 nm as a function of forward pump power when the backward pump power is fixed at ~850 mW.

operation out to 2300 nm, CW lasing at 2315 nm requires higher backward pump power to be initiated under the same forward pump power, and vice versa. Moreover, the output slope efficiency at 1895 nm is higher than that at 2315 nm. On the other hand, Q-switched lasing at 1895 nm and 2315 nm begin simultaneously as the pump powers increase further. Figs. 2(b) and 2(c) show the variations of the central lasing wavelengths at 1895 nm and 2315 nm as a function of the forward pump power for a fixed backward pump power of ~850 mW. As the forward pump power increases, the central wavelengths both increase, indicating that higher pump powers stimulate emission toward longer wavelengths. Finally, both lasing wavelengths approach and maintain around 1895 nm and 2315 nm as the gain at these two wavelengths is substantially saturated.

Fig. 3 shows a typical optical spectrum of the Q-switched output when the forward and backward pump powers are both ~850 mW. The two lasing lines are at 1895.2 nm and 2314.6 nm with full-width at half-maximum (FWHM) bandwidths of ~0.06 nm and ~0.08 nm, respectively, demonstrating the ultra-broadband operation of the graphene SA (~420 nm wavelength separation).

As the pump powers increase, Q-switching operation at 1895 nm and 2315 nm continues with a synchronized rate. For example, when the forward and backward pump powers are both fixed at ~850 mW, the combined and individual pulse trains at 1895 nm and 2315 nm coincide with each other with the same pulse separation of 57.5 μs as shown in Fig. 4. No amplification modulation is observed in each pulse, demonstrating the absence of self-mode-locking effects in Q-switching operation. The synchronized Q-switching opera-

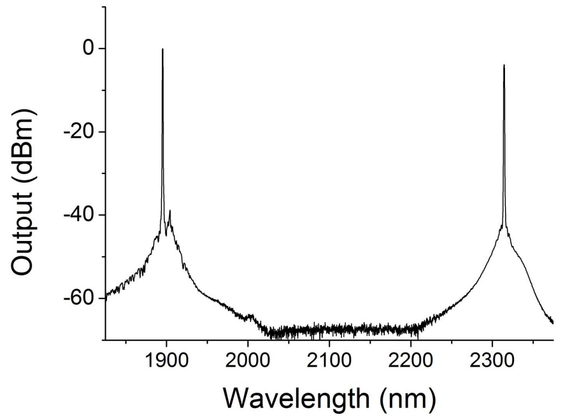

Fig. 3. Optical output spectrum of the graphene Q-switched Tm^{3+}:ZBLAN fiber laser when the forward and backward pump powers are both ~850 mW.

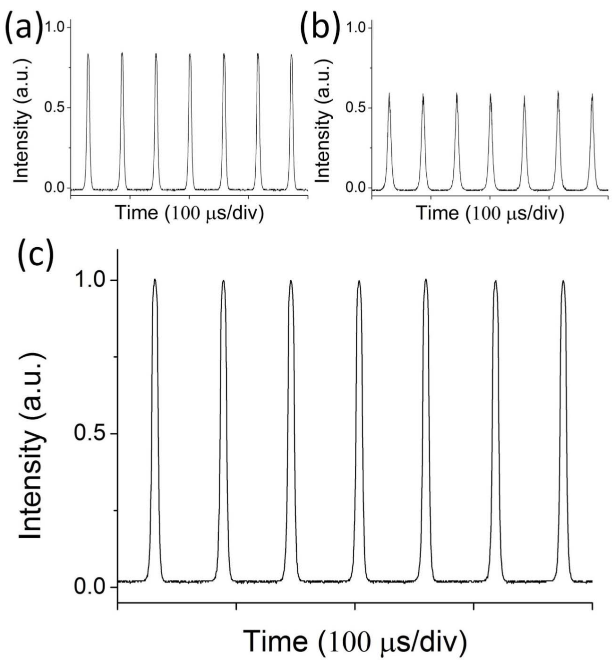

Fig. 4. Q-switched pulse trains at (a) 1895 nm, (b) 2315 nm, and (c) both 1895 nm and 2315 nm when the forward and backward pump powers are both ~850 mW.

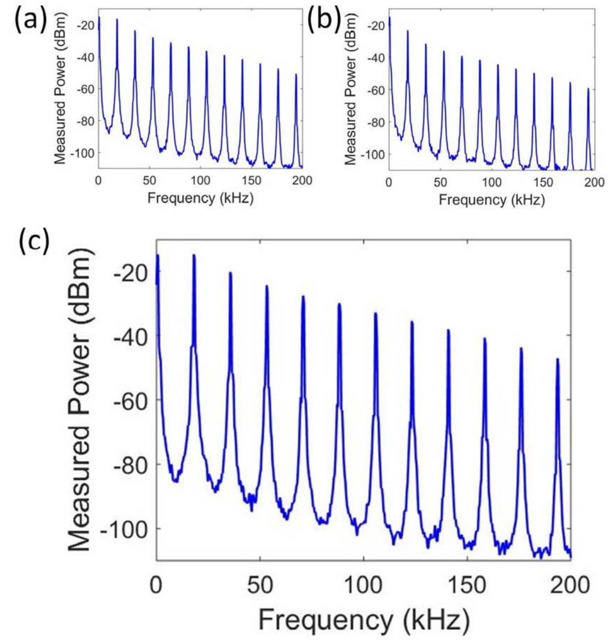

Fig. 5. RF-spectra of the Q-switched laser operating at (a) 1895 nm, (b) 2315 nm, and (c) both 1895 nm and 2315 nm when the forward and backward pump powers are both ~850 mW. Resolution bandwidth = 200 Hz.

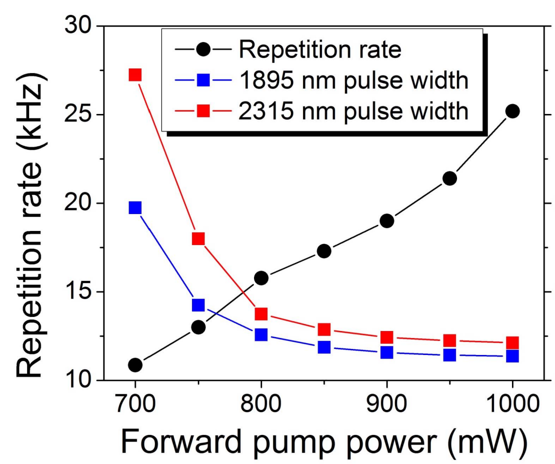

Fig. 6. Repetition rate and pulse width of the Q-switched pulses at 1895 nm and 2315 nm as a function of forward pump power when the backward pump power is ~850 mW.

tion is further demonstrated in the corresponding RF spectra shown in Fig. 5. These three RF spectra show the same repetition rate of ~17.4 kHz. Moreover, the fundamental frequency and harmonics have very high SNR and narrow bandwidth (the 3 dB bandwidth of the peaks is ~300 Hz when measured using a resolution bandwidth of 50 Hz) and there is an absence of peaks at other frequencies which would be present if the two trains had different repetition frequencies.

Fig. 6 shows the pulse repetition rate and the pulse width at each wavelength measured at different forward pump powers when the backward pump power is fixed at ~850 mW. As the forward pump power increases from 700 mW up to 1000 mW, synchronized repetition rate (black dots) increases linearly from 10.8 kHz to 25.2 kHz at a rate of 48 Hz/mW, a typical signature of Q-switching operation. The corresponding pulse widths at 1895 nm (blue square) and 2315 nm (red square) both decrease exponentially first, then keep a level of ~4.5 μs due to the bleaching effect of graphene. The corresponding average output powers and the calculated pulse energies as a function of the forward pump power are shown in Fig. 7. CW lasing at 1895 nm starts at the forward pump power of ~550 mW with a slope efficiency of 0.36%, while CW lasing at 2315 nm starts at the forward pump power of ~650 mW with a slope efficiency of 0.22%, due to the lower cavity loss at 1895 nm. For the range of pump powers used in these experiments, we do not observe any saturation in the output pulse energies, as was the case in [13]. We believe that if the glue splicing can handle higher power, higher repetition rate and higher pulse energies could be observed when higher pump powers are added to the system. At a pump power of 1000 mW for each pump, the average output powers at

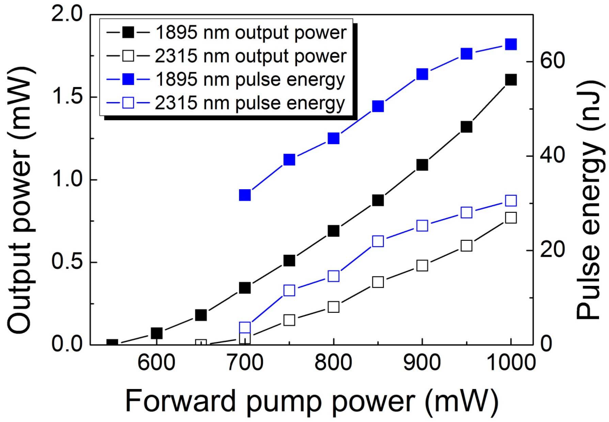

Fig. 7. Output power and pulse energy of the Q-switched pulses at 1895 nm and 2315 nm as a function of forward pump power when the backward pump power is ∼850 mW.

1895 nm and 2315 nm after filtering are 1.6 mW and 0.8 mW, respectively, while the calculated pulse energies are 63.7 nJ and 30.6 nJ, respectively. The corresponding peak powers could reach 13.3 mW and 5.92 mW, respectively.

We believe that we can improve the output power and efficiency of the laser further by reducing the cavity loss. The cavity loss is high due to glue splicing loss between ZBLAN and silica fibers, the coupling loss from the two 795/2000 nm WDM couplers, and the use of SMF-28-based components (which are the only ones available to us in our lab). First, we can replace glue spicing with laser splicing [18] or filament splicing. Second, we can replace the SMF-28-based components (circulator, optical coupler, and fiber on which the graphene SA is deposited) by those based on SM2000 fiber (to reduce transmission losses). Finally, we can also use a separate amplifier to increase further the average output power from the laser.

IV. Conclusion

In conclusion, we demonstrate for the first time a passively Q-switched Tm^{3+}:ZBLAN all fiber laser at 1895 nm and 2315 nm using a single linear cavity and a graphene SA. Q-switched co-lasing operation is obtained with a synchronized repetition rate from 10.8 kHz to 25.2 kHz under a bidirectional pumping scheme at 795 nm, with pulse durations as short as 4.5 μs at 1895 nm and 4.9 μs at 2315 nm. The maximum output powers at 1895 nm and 2315 nm are 1.625 mW and 0.77 mW, respectively, with corresponding calculated pulse energies of 63.7 nJ and 30.6 nJ, and corresponding peak powers of 13.3 mW and 5.92 mW, respectively. Such a dual band Q-switched laser around 1900 nm and 2300 nm could become a low-cost and convenient nanosecond pulse source for applications on the newly exploited optical transmission window around 2000 nm, along with mid-IR dual-band pulse source for the chemical sensing measurements.

References

[1] X. Zhu and N. Peyghambarian, "High-power ZBLAN glass fiber lasers: Review and prospect," *Adv. Optoelectron.*, vol. 2010, pp. 501956-1–501956-23, Jan. 2010.

[2] S. D. Jackson, "Towards high-power mid-infrared emission from a fibre laser," *Nature Photon.*, vol. 6, pp. 423–431, Jun. 2012.

[3] F. J. McAleavey, J. O'Gorman, J. F. Donegan, B. D. MacCraith, J. Hegarty, and G. Mazé, "Narrow linewidth, tunable Tm^{3+}-doped fluoride fiber laser for optical-based hydrocarbon gas sensing," *IEEE J. Sel. Topics Quantum Electron.*, vol. 3, no. 4, pp. 1103–1111, Aug. 1997.

[4] J. N. Carter, R. G. Smart, A. C. Tropper, and D. C. Hanna, "Thulium-doped fluorozirconate fibre lasers," *J. Non-Crystalline Solids*, vol. 140, pp. 10–15, Jan. 1992.

[5] V. Sudesh and J. A. Piper, "Spectroscopy, modeling, and laser operation of thulium-doped crystals at 2.3 μm," *IEEE J. Quantum Electron.*, vol. 36, no. 7, pp. 879–884, Jul. 2000.

[6] R. G. Smart, J. N. Carter, A. C. Tropper, and D. C. Hanna, "Continuous-wave oscillation of Tm^{3+}-doped fluorozirconate fibre lasers at around 1.47 μm, 1.9 μm and 2.3 μm when pumped at 790 nm," *Opt. Commun.*, vol. 82, nos. 5–6, pp. 563–570, May 1991.

[7] S. T. Davey, "Highly efficient and tunable operation of two colour Tm-doped fluoride fibre laser," *Electron. Lett.*, vol. 28, no. 7, pp. 671–673, Mar. 1992.

[8] F. Bonaccorso, Z. Sun, T. Hasan, and A. C. Ferrari, "Graphene photonics and optoelectronics," *Nature Photon.*, vol. 4, no. 9, pp. 611–622, Sep. 2010.

[9] A. Martinez and Z. Sun, "Nanotube and graphene saturable absorbers for fibre lasers," *Nature Photon.*, vol. 7, pp. 842–845, Oct. 2013.

[10] S. Liu *et al.*, "Graphene Q-switched Ho^{3+}-doped ZBLAN fiber laser at 1190 nm," *Opt. Lett.*, vol. 40, no. 2, pp. 147–150, Jan. 2015.

[11] G. Zhu, X. Zhu, K. Balakrishnan, R. A. Norwood, and N. Peyghambarian, "Fe^{2+}:ZnSe and graphene Q-switched singly Ho3+-doped ZBLAN fiber lasers at 3 μm," *Opt. Mater. Exp.*, vol. 3, no. 9, pp. 1365–1377, Sep. 2013.

[12] C. Wei *et al.*, "Graphene Q-switched 2.78 μm Er^{3+}-doped fluoride fiber laser," *Opt. Lett.*, vol. 38, no. 17, pp. 3233–3236, Aug. 2013.

[13] C. Jia *et al.*, "Passively synchronized Q-switched and mode-locked dual-band Tm^{3+}:ZBLAN fiber lasers using a common graphene saturable absorber," *Sci. Rep.*, vol. 6, p. 36071, Nov. 2016.

[14] J. Li *et al.*, "Mid-infrared passively switched pulsed dual wavelength Ho^{3+}-doped fluoride fiber laser at 3 μm and 2 μm," *Sci. Rep.*, vol. 5, p. 10770, Jun. 2015.

[15] Z. Li, A. M. Heidt, J. M. O. Daniel, Y. Jung, S. U. Alam, and D. J. Richardson, "Thulium-doped fiber amplifier for optical communications at 2 μm," *Opt. Exp.*, vol. 21, no. 8, pp. 9289–9297, Apr. 2013.

[16] B. J. Shastri, M. A. Nahmias, A. N. Tait, A. W. Rodriguez, B. Wu, and P. R. Prucnal, "Spike processing with a graphene excitable laser," *Sci. Rep.*, vol. 6, p. 19126, Jan. 2016.

[17] Z. Luo *et al.*, "Graphene-based passively Q-switched dual-wavelength erbium-doped fiber laser," *Opt. Lett.*, vol. 35, no. 21, pp. 3709–3711, Nov. 2010.

[18] J. H. Chong, M. K. Rao, Y. Zhu, and P. Shum, "An effective splicing method on photonic crystal fiber using CO_2 laser," *IEEE Photon. Technol. Lett.*, vol. 15, no. 7, pp. 942–944, Jul. 2003.